Dynamical Climatology

The response of a simple thermodynamic sea-ice model to GCM forcing appropriate for perennial sea-ice.

by

M. Bottomley

DCTN 3 September 1984

Meteorological Office (Met. O. 20)
London Road
Bracknell
Berkshire RG12 2SZ

DYNAMICAL CLIMATOLOGY TECHNICAL NOTE NO 3

THE RESPONSE OF A SIMPLE THERMODYNAMIC SEA-ICE MODEL TO GCM FORCING APPROPRIATE FOR PERENNIAL SEA-ICE

by

M. BOTTOMLEY

Met O 20 (Dynamical
Climatology Branch)
Meteorological Office
London Road
Bracknell
Berkshire RG12 2SZ

September 1984

Note: This paper has not been published. Permission to quote from it should be obtained from the Assistant Director of the above Meteorological Office Branch.

1. Introduction

A single column model describing the thermodynamic growth and decay of sea-ice in response to energy fluxes at the upper and lower boundaries has been developed for use in climate studies. This note compares the response of the model to zonal mean forcing derived from a seasonal integration of the 5-layer atmospheric model (5LM) with that using climatological values characteristic of perennial Arctic sea ice.

2. Formulation of the model

The ice model is based on Semtner's zero-layer model (Semtner, (1976)) in which the surface temperature, T_S, of a combined snow-ice layer (Fig 1) is determined from a flux balance condition at the upper surface. The internal snow-ice temperature structure is not monitored directly. Instead a linear temperature gradient is assumed between the surface and the lower boundary. The resulting uniform heat flux through the combined layer is given by:

$$F_S = \frac{k_S (T_B - T_S)}{h_S + \frac{k_S}{k_I} . h_I} \qquad (2.1)$$

which, for snow-free ice, reduces to

$$F_S = \frac{k_I (T_B - T_S)}{h_I} \qquad (2.2)$$

where k_S and k_I are the thermal conductivities of snow and ice respectively; h_S and h_I are, respectively, the snow depth and the ice depth; T_B is the temperature at the lower boundary which is held fixed at the freezing point of sea water (271.2K).

Since the diffusion of heat through snow or ice is governed by an equation of the form

$$\rho c \frac{\partial T}{\partial t} = \frac{\partial}{\partial z}\left(k \frac{\partial T}{\partial z}\right) \qquad (2.3)$$

where ρ, c and k are the appropriate density, specific heat capacity and thermal conductivity, respectively, $T = T(z)$ is the temperature within the snow or ice and z is the vertical coordinate, the assumption of a linear temperature gradient is equivalent to the neglect of heat capacity. No energy is required, then, to warm the interior of the ice prior to melting in spring and neither is any interior cooling necessary before the onset of freezing in the autumn. Semtner's zero layer model gives a lower equilibrium annual mean ice depth than his multi-layer model - a fact which he attributed to the neglect of heat capacity. To compensate for this Semtner increased k_S and k_I (usually 0.31 and 2.03 $Jm^{-1}s^{-1}K^{-1}$ respectively) by a factor $\gamma = 1.065$. (Semtner, (1976)).

The surface temperature is obtained from a flux balance condition:

$$F_A + F_S = 0 \qquad (2.4)$$

where F_A is the net downward flux from the atmosphere:

$$F_A = (1-\alpha) F_{SW} + F_{LW} - \varepsilon \sigma T_S^4 + F_{SH} + F_{LH} \qquad (2.5)$$

and F_{SW} represents the flux of incoming solar short-wave radiation,

αF_{SW} the reflected short-wave (SW) radiation,

α the surface (snow or ice) albedo,

F_{LW} the flux of incoming long-wave radiation,

$\varepsilon \sigma T_S^4$ the outgoing long-wave (LW) radiation,

ε the long-wave emissivity,

σ the Stefan-Boltzmann constant,

F_{SH} the downward flux of sensible heat,

F_{LH} the downward flux of latent heat.

Note that Semtner defines F_A to be the net upward flux.

For consistency with Maykut and Untersteiner's calculations Semtner used the value $\sigma = 5.797 \times 10^{-8}$ W m^{-2} K^{-4}. However this is about 2% higher than is generally accepted (e.g. Kaye and Laby (1973) give σ = 5.669×10^{-8} W m^{-2} K^{-4}) and, as discussed in section 4, this has a substantial effect on the model results. In our calculations the value used in the 5LM ie $\sigma = 5.66985 \times 10^{-8}$ Wm^{-2}K^{-4} was adopted and, following Semtner and Maykut and Untersteiner, the long-wave emissivity, ε, was taken to be unity.

Penetrative radiation, which warms the subsurface interior of the ice and enlarges the brine pockets trapped within it, cannot be represented explicitly in the model since both the thermal capacity of the ice and the storage of latent heat in brine pockets are neglected. Following Semtner (1976) the effects of penetrative radiation - primarily a reduction in the amount of heat available for surface melting and an increase in annual mean ice thickness (see Table 3, Semtner (1976)) - are allowed for by reflecting away a portion β of the radiation which is assumed would otherwise

penetrate into the interior of the (snow-free) ice, and making the remainder available for surface melting. This is achieved by the use of an enhanced ice albedo, i.e.

$$\alpha = \alpha_I + \beta (1-\alpha_I) I_o \qquad (2.6)$$

where α_I is the bare ice albedo,

I_o is the fraction of SW radiation which penetrates the snow-free ice surface. (I_o = .17 in the calculations described in this note).

Semtner found that the value β = 0.4 gave the correct annual mean ice depth. However the phase and amplitude of the seasonal range of ice thickness were not in agreement with those predicted by multi-level models. (Semtner, 1976).

Two of the terms in Eqn. (2.4) are temperature dependent. The value of T_S which satisfies this balance condition is obtained numerically by expressing the surface temperature as $T_S = T_P + \Delta T$ (where T_P is the value of the surface temperature at the previous time step) to give a linear approximation to the black body emission term $\varepsilon\sigma T_S^4$). The flux balance condition thus becomes

$$(1-\alpha) F_{SW} + F_{SH} + F_{LH} + F_{LW} - \varepsilon\sigma T_P^4 - 4\varepsilon\sigma T_P^3 \Delta T + \frac{k_S (T_B - T_P - \Delta T)}{h_S + h_I \cdot \frac{k_S}{k_I}} = 0 \qquad (2.7)$$

which can be solved for ΔT and therefore T_S.

If the predicted surface temperature exceeds the melting point (273.15K for snow-covered ice, 273.05K for snow-free ice) it is reset to the melting point. This causes an imbalance in the fluxes through the surface when the temperature dependent terms are recomputed. The resulting excess energy is used to melt some of the snow cover, or some of the ice itself once the surface is snow-free, according to

$$\Delta h_S = -\frac{\Delta t}{q_S}\left(F_A + F_S\right) \qquad (2.8)$$

or

$$\Delta h_I = -\frac{\Delta t}{q_I}\left(F_A + F_S\right), \qquad (2.9)$$

where q_S and q_I are the heats of fusion of snow and ice respectively. Following Semtner, we use the values $q_S = 1.097 \times 10^8$ Jm^{-3} and $q_I = 3.014 \times 10^8$ Jm^{-3}.

The ice thickness also changes by ablation or accretion at the lower boundary according to the imbalance between the specified upward oceanic heat flux, F_B, and the diffusive heat flux, i.e.

$$\Delta h_B = \frac{\Delta t}{q_B}\left(F_S - F_B\right) \qquad (2.10)$$

where q_B is the latent heat of fusion of ice at the lower boundary. To allow comparison with the results of Maykut and Untersteiner's experiments, Semtner (1976) used a lower value for the latent heat of fusion of ice at the lower boundary than at the surface. However this model, unlike Maykut and Untersteiner's, does not represent the effects of salinity and so we have used identical values of q at the two boundaries i.e. $q_B = q_I$.

If the thickness changes Δh_I and Δh_B combine to give open water i.e. $h_I = 0$, the thermal forcing is then applied to a simple ocean mixed layer (30m deep) whose temperature change is determined from a heat budget equation:

$$\Delta T_W = \frac{[(1-\alpha)F_{SW} + F_{LW} + F_{SH} + F_{LH} - \varepsilon\sigma T_W^4 + F_B]}{c_W \cdot d_{mix}} \quad (2.11)$$

where T_W is the mixed layer temperature,

d_{mix} is the mixed layer depth,

α_W is the albedo of sea water,

c_W is the volumetric heat capacity of water.

When T_W falls below the freezing point of sea water the ice depth is set to an arbitrary value of 1 cm and the equations describing heat transfer through the ice are brought into play again. In order to conserve energy 1 cm of ice is removed, without expenditure of energy, when the ice cover disappears.

If the situation arises in which the predicted ice depth, h_I, falls below 1 cm but a quantity of snow remains, the ice depth is set back to 1 cm by conversion of an appropriate amount of snow ($\frac{0.90}{0.33}(0.01 - h_I)$ m).

For consistency with the work of Maykut and Untersteiner (1971), and Semtner (1976), changes in snow/ice depth due to sublimation and evaporation were neglected in the experiments described here. When the model is used in GCMs however, these effects will be included.

3. Comparison of GCM and observed climatological forcing parameters.

In subsequent sections the response of the ice model to forcing data extracted from an annual cycle run (experiment 767) of the 5 layer model (5LM) (Slingo, 1982) is examined. First, however, the 5LM albedo formulation and the 5LM forcing for days 310 to 674 of exp 767 are compared with the albedo formulation and the climatologically observed forcing used both by Semtner (1976) and Maykut and Untersteiner (1971). The forcing prescribed by these authors (Table I) is based on monthly average values taken from Fletcher (1965) and is appropriate to conditions over perennial Arctic sea ice. Figures 2-4 compare the zonal monthly means of the total incoming solar radiation at the ground (including the contribution due to reflection from clouds), the incoming long-wave radiation and the sum of the sensible and latent heat fluxes for the permanent ice points of Rows 1-4 of the 5LM with the corresponding quantities in Fletcher's heat budget (Table I). Rows 1-4 of the 5LM span the latitude band 88.5°N to 79.5°N. It is noted here that sea ice in the 5LM is treated as a slab of constant 2m thickness (see for example Corby, Gilchrist and Rowntree, 1977) whose spatial distribution is prescribed from climatology and allowed to vary accordingly through the annual cycle.

Since values of the incoming solar radiation, F_{SW}, for the 5LM were not directly available from the model output they were derived from the net solar radiation at the surface, F_{SW}^{Net}, averaged for each day by setting

$$F_{SW} = \frac{F_{SW}^{Net}}{1 - \alpha}$$

where α is the prescribed albedo for the ice surface. The 5LM takes the ice albedo to be 0.8 for an ice surface temperature of less than 271.2K and 0.5 for an ice surface temperature greater than this value. The lower value of albedo chosen for surface temperatures greater than 271.2K is intended primarily to reflect the presence of liquid water (melt ponds) on the ice surface, although an albedo change at 273.15 would seem more appropriate for this.

Semtner and Maykut and Untersteiner derive the albedo of snow-covered ice from the monthly mean values reported by Marshunova (1961). These are given in Table I. Semtner also assumes that, at the onset of melting, the albedo decreases linearly with snow depth to the bare ice value of 0.64.

With the exception of a short period around July and August monthly mean values of 5LM incoming SW radiation are seen to be less than those given by Fletcher (Fig. 2). The discrepancy is as much as 30-40 Wm^{-2} in June. This is probably due to the fact that the low cloud albedo in the 5LM is too high for Arctic stratus (the predominant cloud type in the Arctic) (Herman and Curry, 1984; J M Slingo, 1982).

The 5LM incoming LW radiative flux is seen (Fig 3) to be significantly lower than the climatological values through much of the year. The difference exceeds 60 Wm^{-2} in September. This may be due in part to (i) neglect of the temperature dependence of the fraction of black body flux allocated to each spectral band, and (ii) the treatment of emission and absorption by the water vapour continuum (Slingo and Wilderspin, 1984).

The combined sensible and latent heat fluxes (Fig. 4) show quite good agreement, with the exception of late summer and autumn values on Row 4.

Snow is assumed by Semtner (following Maykut and Untersteiner) to fall at a rate of 30 cm between August 20 and October 30, 5 cm between November 1 and April 30, and 5 cm in May. This may be compared with 5LM monthly mean snowfall for Rows 1-4 by reference to Fig. 5. Annual snowfall totals are given in Table II. According to Maykut and Untersteiner snowfall in the central Arctic is low over most of the year but has two peaks - one in May and a very large peak in the autumn. GCM snowfall for the corresponding region is rather more evenly distributed and reaches an autumn maximum of about 0.5 mm water equivalent/day only (on Row 4).

4. The standard integration

In sections 4-6 we shall compare the behaviour of the ice model when run with 5LM forcing, with a standard integration which is the equivalent of Semtner's Case 1 (i.e. Fletcher's forcing, $F_B = 2$ Wm^{-2}, $I_o = 17\%$, 8 hour timestep) (Semtner, (1976)) but with:

(i) the modified value of σ described previously (see Section 2),

(ii) identical latent heats of fusion at the upper and lower boundaries (see Section 2),

(iii) no oceanic heat flux i.e. $F_B = \phi.$,

(iv) 24 hour timestep.

It should first be noted however that with our version of the model and, like Semtner, a timestep of 8 hours the Case 1 integration gives an equilibrium annual mean ice depth of 2.93m (c.f. Semtner's 2.89m). With a 24 hour timestep the equilibrium annual mean depth increases to 2.97m.

The use of the lower value of σ has a substantial effect on the equilibrium annual mean ice depth, reducing it from 2.97m to 1.73m. This may be accounted for in terms of differences in summer ablation, primarily at the surface of the ice. Fig. 6 shows the evolution of monthly mean ice depth and surface temperature in the first year of the two integrations, starting from identical initial conditions. For most of the year the surface temperature in the integration with the standard value of σ exceeds that in the integration using Semtner's value. This counterbalances the effect of the lower value of σ on the outgoing LW radiation ($\varepsilon\sigma T_s^4$ term in Eqn. (2.5)) and consequently, ice accumulation rates during September - May are very similar. The only significant divergence in the monthly mean ice depths occurs during the melt season (June - Aug) when the surface temperature is held at the melting point in both integrations. The effect of the lower value of σ is then apparent i.e. outgoing LW radiation is reduced so that more energy is available for surface ablation. Furthermore since the use of the standard value of σ accelerates the removal of the snow cover once the melt season is under way, the ice is snow-free for a longer period (7 days longer in the 1st year). This further enhances the subsequent surface ablation because of the lower albedo of bare ice compared with that of snow-covered ice. The importance of enhanced surface ablation in the reduction of the annual mean ice depth is apparent in Fig. 7 which shows the contribution to the total change in ice depth from surface ablation and from bottom ablation/accretion in the two integrations. Amounts of bottom ablation/accretion are similar throughout the year whereas there is a large difference in surface ablation in summer.

Fig. 7 also shows that accretion dominates ablation at the lower boundary. Therefore, since increasing q_B reduces the magnitude of the change Δh_B (see Eqn (2.10)) the net effect of the larger value of q_B is a reduction in ice depth. The equilibrium annual mean ice depth obtained using both the accepted value of σ and $q_B = q_I = 3.014 \times 10^8$ Jm^{-3} is 1.36m.

This value may be compared with observed depths in the central Arctic of between 2.5m and 3.5m. As the actual magnitude of the oceanic heat flux, F_B, is not well known it could be argued that the 2 Wm^{-2} used in Semtner's Case 1 integration might be inappropriate for the central Arctic. However, as Fig 8 shows, a flux from the ice to the ocean below (~ 1 Wm^{-2}) would be necessary to achieve a depth within the range quoted above (and this would require that the ocean temperature be less than 271.2K, the freezing point temperature). Consequently the value $F_B = 0$, which gives an equilibrium annual mean ice depth of 2.30m, was adopted for our standard integration.

Fig 9 shows the evolution of ice depth in the standard integration from initially prescribed ice and snow depths of 2m and 0m respectively, and a surface temperature of 242K. With these initial conditions the model takes some 18 years to come to equilibrium i.e. to achieve a constant cycle of ice depth (to the nearest centimetre). The equilibrium annual cycles of surface temperature, ice thickness and snow cover are shown in more detail in Figures 10a and 10b. As would be expected the ice thickness increases from early autumn to late spring and decreases when the surface temperature rises to the melting point during the summer months. Figure 10c shows a plot of the total monthly changes in ice thickness and Figure 10d the contributions to the total from bottom ablation/accretion and surface ice

melt. As dictated by Eqns (2.1) and (2.10) growth occurs through bottom accretion from early autumn to late spring when the surface temperature is below freezing for sea water. (Since $F_B = 0$ in this case the requirement that the magnitude of the upwards heat flux through the ice, F_S, should exceed the oceanic heat flux, F_B, for accretion is always met). Water is frozen to the bottom of the ice to maintain the heat balance at the lower boundary. Through the summer months, when the surface temperature rises to the fresh water melting point (which exceeds that of saline sea ice so that the conductive heat flux is downwards), there is a convergence of heat at the lower boundary and a small amount of bottom ablation takes place. Most of the depletion of the ice, however, occurs as a result of surface melting once the snow cover has itself, melted away. The ice assumes its equilibrium cycle when the ice growth by bottom accretion through the winter months (which decreases as the ice thickens (Eqns (2.1) and (2.10)) balances the summer ablation.

5. Integrations with GCM snowfall or albedo

(5.1) Standard integration with GCM snowfall.

The total annual snowfall for Rows 1-4 of the 5LM is significantly less than in the standard integration. This difference is reflected in the equilibrium annual mean ice depths obtained using GCM snowfall in otherwise standard integrations (Table II). With a thinner cover of insulating snow surface temperatures are reduced, thereby increasing the upwards heat flux through the ice/snow layer. This promotes accretion of ice at the lower boundary and greater ice depths result. (Although Row 1 has both a higher total annual snowfall and a greater ice depth than say Row 3, the snowfall distributions are different in the two cases. On Row 1 a significant

proportion (almost 30%) of the total snowfall occurs during the months June - August when both the surface and the lower boundary are melting. This snow does not accumulate, nor is the latent heat needed to melt it taken into account (consistent with Semtner's treatment), and so it does not contribute to the insulation of the ice during the winter months. On Row 3, on the other hand, only 10% of the total falls during these months).

(5.2) Standard integration with 5LM albedo.

The 5LM albedo formulation involves a reduction in the albedo value during the summer melt season i.e. $\alpha = 0.5$ when $T_S > 271.2$ compared with the (bare ice) value of $\alpha = 0.64$ in Semtner's calculation (see Section 3). The associated increase in net short wave radiation, and thereby in surface ablation, results in a very much reduced equilibrium annual mean ice depth (0.90m) compared with the standard integration (2.30m). As lower ice depths promote winter accretion the ice growth rate is increased (Fig 11a). This, with the enhanced surface ablation in the summer months, increases the seasonal range of ice depth from 0.8m in the standard integration to 1.8m.

A further consequence of the enhanced surface ablation is the appearance of open water. Equation (2.1) shows that as the ice gradually melts away F_S increases. Therefore the heat loss from the surface increases and this eventually brings about an early end to surface ablation, despite the enhanced net short wave radiation available. In fact the surface temperature drops below melting point on Aug 12 - some 14 days ahead of the standard integration. The ice cover remains at this stage but is only a few centimetres thick and consequently F_S (which is still directed downwards through the ice since $T_S > 271.2$) is an order of

magnitude larger than in the standard integration. Bottom ablation continues after the end of surface melting and it is this which erodes the final few centimetres of ice and brings about the formation of open water (which survives until the middle of October).

This rather unusual sequence of events - the onset of a prolonged period of open water after surface melting has ceased and surface temperatures are starting to fall - is only an artefact of the model which maintains different melting points at the upper and lower boundaries even when the ice is very thin. Furthermore, dynamical effects and the presence of leads (areas of open water within the ice pack) - which are not represented in the model - will play an important role in the removal of thin ice to form open water.

6. Integrations with GCM forcing

We have seen in Figs 2 and 3 that zonally meaned incoming SW and incoming LW radiation derived from the 5LM for Rows 1-4 are usually less than the corresponding climatological value. The experiments described here using 5LM fluxes appropriate for Row 1 - with both the 5LM and Semtner's albedo formulation - indicate that this would be a serious handicap in global simulations, as the amount of surface ablation that can take place is severely restricted.

(6.1) Row 1 atmospheric fluxes and snowfall; Semtner albedos

According to Semtner's formulation the albedo values gradually decrease during the spring and summer (as the snow depth decreases) thereby increasing the net solar radiation available for surface ablation. With 5LM fluxes this is sufficient to melt all the winter snow cover each year but only a few centimetres of ice. At the lower boundary net ablation of

ice only occurs during July when the surface temperature remains in excess of 271.2K for a sufficiently long period. Throughout the rest of the year ice accretion dominates (note again that since $F_B = 0$ accretion occurs whenever the conductive heat flux is directed upwards through the ice i.e. $T_S < 271.2K$). Thus, with an insignificant amount of surface ablation, the ice depth steadily increases and by the end of the integration (50 years) has reached a wholly unrealistic (and still increasing) depth of 21.73m.

The variation in surface temperature during this final year is compared with the equilibrium variation in the standard integration in Fig 12. With the exception of the melting period, T_S is significantly lower (~ 10K) than in the standard integration. This is a direct consequence of the lower forcing fluxes.

The small maximum in T_S in November reflects a similar maximum in the combined GCM forcing fluxes at this time.

(6.2) Row 1 atmospheric fluxes and snowfall; 5LM albedos

Although the 5LM albedo formulation involves a potentially smaller albedo than Semtner's formulation during the summer months (0.5 c.f. 0.64), the surface temperature never reaches 271.2K in this calculation and therefore the reduction in albedo cannot take place. There is no surface ablation - neither of snow nor of ice - and the snowfall merely accumulates on the surface. Furthermore with $T_S < 271.2K$ and $F_B = 0$ there is no bottom ablation either, so that both snow and ice depths increase throughout the integration. The rate of increase of ice depth is less than in the corresponding integration with Semtner's albedo formulation ((a) above), however, because of the very deep snow cover insulating the ice. The annual mean ice and snow depths at the end of the integration (year 50) are 13.04m and 10.48m respectively.

(6.3) Rows 54,55,56 atmospheric fluxes and snowfall; 5LM albedos

Annual mean ice and snow depths obtained in the final year of calculations similar to that described in (6.2) but with GCM surface fluxes and snowfall appropriate for those southern hemisphere rows consisting entirely of permanent ice points (Rows 54-56) are given in Table III. These calculations show the same features as the calculation with Row 1 fluxes i.e. the absence of both surface and bottom ablation, and the excessive accumulation of snow. It should be noted however that the zero oceanic heat flux was introduced in order to match model results, using climatological forcing, to observations in the central Arctic. There is, therefore, no real basis for its use in the southern hemisphere. Using a similar model, Parkinson and Washington (1979) found that an oceanic heat flux of 25 Wm^{-2} was necessary to obtain reasonable results in the Antarctic.

7. Sensitivity to bottom heat flux

The variation of the equilibrium annual mean ice depth with oceanic heat flux in the standard integration has already been referred to in Section 4. As Fig 8 showed ice depths decrease with increasing F_B. With no heat flux from the ocean, bottom accretion occurs whenever the surface temperature is below 271.2K whereas with $F_B > 0$ the requirement that $F_S > F_B$ must also be met. ie. F_S must be large enough to counteract the influence of the heat flux from the ocean. Therefore, in addition to the enhanced ablation associated with increasing F_B, the amount of winter ($T_S < 271.2$) accretion is diminished. Both effects, of course, bring about lower ice depths.

The value of the bottom heat flux has a marked effect on the sensitivity of the model results to other forcing parameters.

(i) Snowfall

We have seen that reducing snowfall, and thereby snowdepth h_S, increases the upwards heat flux through the ice and that this in turn promotes winter accretion of ice. The heat flux through the ice is inversely related to both snow depth and ice depth, h_I (see Eqn 2.1). For any given ice depth, then, (and assuming a constant surface temperature) the rate of change of F_S with h_S, $\left(\frac{\partial F_S}{\partial h_S}\right)_{h_I, T_S}$ is proportional to $-\frac{1}{(h_S + \frac{k_S}{k_I} \cdot h_I)^2}$. Therefore as h_I is reduced the sensitivity of F_S to variations in h_S is enhanced. In other words, the effect of variations in snowfall are more apparent in the model results as F_B is increased. The effect of varying snowfall amounts in calculations made with $F_B = 2.0$ Wm^{-2} is compared with that observed in the corresponding calculations made with $F_B = 0.0$ Wm^{-2} in Table III. Fig. 13 illustrates the sensitivity of the model to snowfall over a range of F_B.

(ii) Atmospheric fluxes from GCM

The results of increasing the upwards oceanic heat flux from $F_B = 0.0$ Wm^{-2} to $F_B = 2.0$ Wm^{-2} in the experiments using GCM atmospheric fluxes are also given in Table III.

The characteristic effect of using the 5LM fluxes is the inhibition of surface ablation so that changes in ice depth occur primarily at the lower boundary (see Section 6). For realistic ice and snow depths accretion dominates here. Bottom ablation occurs only when

$$F_S = \frac{k_S (271.2 - T_S)}{h_S + \frac{k_S}{k_I} \cdot h_I} < F_B \quad . \qquad (7.1)$$

With $F_B = 0$ this condition can obviously only be satisfied when $T_S > 271.2K$. Since this occurs for short periods only with the GCM forcing - if at all - the ice depth increased throughout the integration (see Section 6). Ice accretion becomes increasingly small however as h_I and/or h_S increase.

For $F_B > 0$ on the other hand, bottom ablation becomes increasingly more significant as the ice and/or snow depth increase. The heat flux, F_S, is particularly sensitive to snow depth since $\frac{k_S}{k_I} \sim .15$. When the 5LM albedo formulation is used snow accumulates on the surface of the ice (since T_S never exceeds 271.2K in this case) and eventually this is sufficient to satisfy (7.1) throughout the year. The ice cover is then gradually eroded from the lower boundary whilst the snow depth continues to increase (see Table III). The amount of snow required to initiate the melting decreases as the oceanic heat flux increases.

Semtner's albedo formulation, on the other hand, allows sufficient surface ablation for an equilibrium annual cycle of snow depth to be established i.e. there is no progressive increase in snow depth. In this case it is the increase in ice depth, which, for $F_B > 0$, increases the likelihood of bottom ablation of ice. Therefore, a negative feedback mechanism operates which will allow the ice depth to reach equilibrium eventually (but only after hundreds of years).

8. Discussion

These experiments have illustrated the high sensitivity of the zero-layer sea-ice model to the forcing fluxes. The quality of simulated ice extents and ice depths in coupled atmosphere-ocean-ice experiments

will, therefore, be strongly dependent on the quality of the radiative and turbulent fluxes obtained from the atmospheric model, the bottom heat flux obtained from the ocean model and the albedo formulation. The incoming radiative fluxes from the 5 layer atmospheric model are known to be too low compared with climatology and this has been seen to restrict the amount of surface ablation that can take place very severely.

The most significant effect on the ice depth of variations in the forcing occurs during the melting season (see Section 4). For most of the year, variations in surface temperature provide a feedback mechanism (through the back long-wave radiation) which tends to counteract the effect of the perturbation. During the melting season however the surface temperature is held fixed and all of the net surface energy is available for surface ablation. It is possible that the representation of the melting process in the model is incomplete. For example no allowance is made, other than in the albedo scheme (see Section 3), for the presence of melt ponds and absorption of energy by these ponds would provide an alternative sink of energy to ice ablation. However there does not seem to be any simple way in which an adequate representation of melt ponds could be incorporated into the model. It is unlikely that development of a complex representation could be justified at this stage, since other processes which can be expected to be of fundamental importance in determining the quality of the simulation of the ice cover - such as ice dynamics - are neglected.

References

Corby, G.A., A. Gilchrist and P.R. Rowntree, 1977, Methods in Computational Physics, 17, 67.

Fletcher, J.O., 1965, The Rand Corporation, Santa Monica, California, R-444-PR.

Herman, G.F., and J.A. Curry, 1984, J. Clim. and Appl. Meteor., 23, 5.

Kaye, G.W.C., and T.H. Laby, 1973, Tables of physical and chemical constants, 14th ed., Longman.

Marshunova, S., 1961, Proc. Arctic and Antarctic Res. Institute No. 229, Leningrad. [Translated by the Rand Corporation, RM-5003-PR, (1966)].

Maykut, G.A., and N. Untersteiner, 1971, J. Geophys. Res., 76, 1550.

Parkinson, C.L., and W.M. Washington, 1979, J. Geophys. Res., 84, 311.

Semtner, J.,Jr., 1976, J. Phys. Oceanogr., 6, 379.

Slingo, A. and R.C. Wilderspin, (in preparation).

Slingo, J.M., (1982), Q.J. Roy. Met. Soc., 108, 379.

	Jan	Feb	Mar	Apr	May	Jun	Jul	Aug	Sep	Oct	Nov	Dec
Incoming short wave radiation (Wm^{-2})	0	0	30.7	159.8	285.8	310.0	219.6	145.3	59.7	6.5	0	0
Incoming long wave radiation (Wm^{-2})	167.9	166.3	166.3	187.3	243.8	290.6	308.4	301.9	266.4	224.4	180.8	176.0
Downward flux of sensible heat (Wm^{-2})	19.0	12.3	11.6	4.7	-7.3	-6.3	-4.8	-6.5	-2.7	1.6	9.0	12.8
Downward flux of latent heat (Wm^{-2})	0.0	-0.3	-0.5	-1.5	-7.4	-11.3	-10.3	-10.7	-6.3	-3.1	-0.2	-0.2

Table I Climatological forcing based on Fletcher's heat budget (Fletcher, 1965) and snow albedos taken from Marshunova (1961) used by Semtner (1976) and Maykut and Untersteiner (1971). Downward fluxes are positive.

	Annual snowfall (cm/year)	Equilibrium Annual Mean Ice Depth (m)
Row 1	21.2	2.59
Row 2	14.1	2.55
Row 3	17.6	2.52
Row 4	28.5	2.40
Standard Integration	39.6	2.30

Table II Comparison of annual snowfall and corresponding equilibrium annual mean ice depth for the standard integration (Maykut and Untersteiner's (1971) snowfall) and similar integrations using GCM snowfall.

Integration	Annual Mean Ice and Snow Depth (Year 50)			
	F_B = 0.0 Wm^{-2}		F_B = 2.0 Wm^{-2}	
Standard	2.30	(0.22)	1.36	(0.22)
Standard + 5LM Snow Row 1	2.59	(0.07)	1.99	(0.07)
Standard + 5LM Snow Row 2	2.55	(0.06)	2.00	(0.06)
Standard + 5LM Snow Row 3	2.52	(0.07)	1.94	(0.07)
Standard + 5LM Snow Row 4	2.40	(0.12)	1.74	(0.12)
Standard + 5LM Albedo	0.90	(0.05)	$\begin{bmatrix}0.90\\0.87\end{bmatrix}^{+}$	$\begin{bmatrix}0.03\\0.03\end{bmatrix}^{+}$
5LM Forcing (Row 1) + Semtner Albedo	21.73†	(0.11)	15.57†	(0.11)
5LM Forcing (Row 1) + 5LM Albedo	13.04†	(10.48†)	3.60*	(10.48†)
5LM Forcing (Row 54) + 5LM Albedo	6.28†	(34.36†)	0.01	(24.14†)
5LM Forcing (Row 55) + 5LM Albedo	7.93†	(26.46†)	0.01	(20.85†)
5LM Forcing (Row 56) + 5LM Albedo	14.09†	(10.41†)	0.01	(10.41†)

Table III Summary of annual mean ice depths (m) in final year of integrations referred to in sections 4–6. Results are also given for corresponding calculations with $F_B = 2.0$ Wm^{-2}. Annual mean snow depths (m) are shown in brackets. The ice and snow depths quoted are equilibrium values unless otherwise indicated. Note that ice depths of 0.01m may be taken as zero since the ice depth is maintained at this depth only by conversion of an appropriate amount of the snow cover.

+ Equilibrium cycle of two-year period.

† Increasing ice/snow depth.

* Decreasing ice/snow depth.

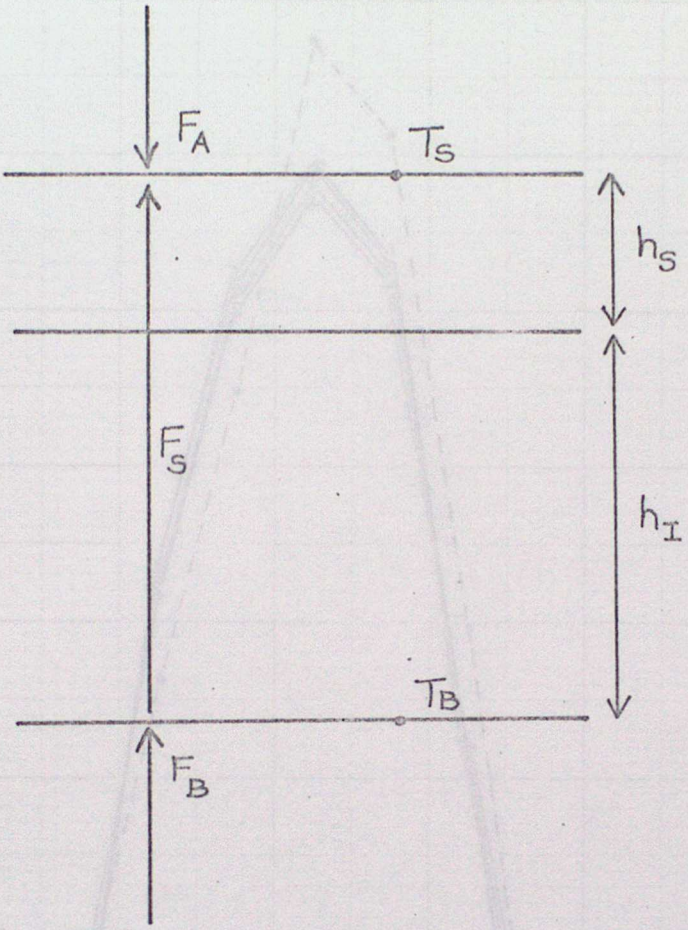

Fig 1: Simple ("zero-layer") ice model.

F_A: Net downward flux from the atmosphere, including contributions from solar and long-wave radiation, sensible and latent heat fluxes.
F_S: Conductive heat flux through the snow/ice system.
F_B: Upward heat flux from the ocean
T_S: Surface temperature
T_B: Lower boundary temperature
h_I: Ice depth
h_S: Snow depth

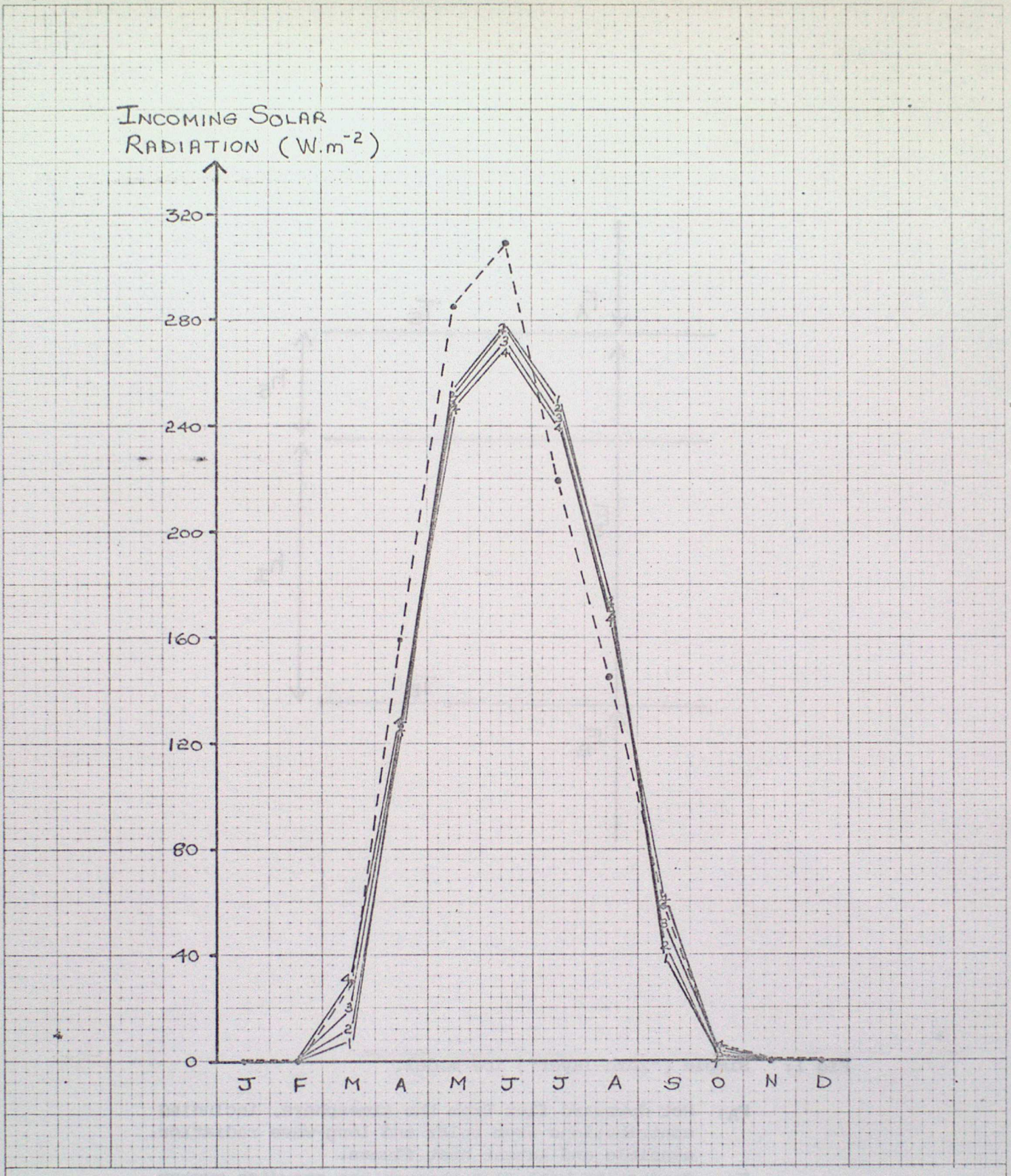

FIG. 2 : Incoming solar radiation

•------• Fletcher (1965). (Conversion from Fletcher's units assumes 30-day means.)

——— Zonal mean values, 5LM Rows 1-4. (Ice points only)

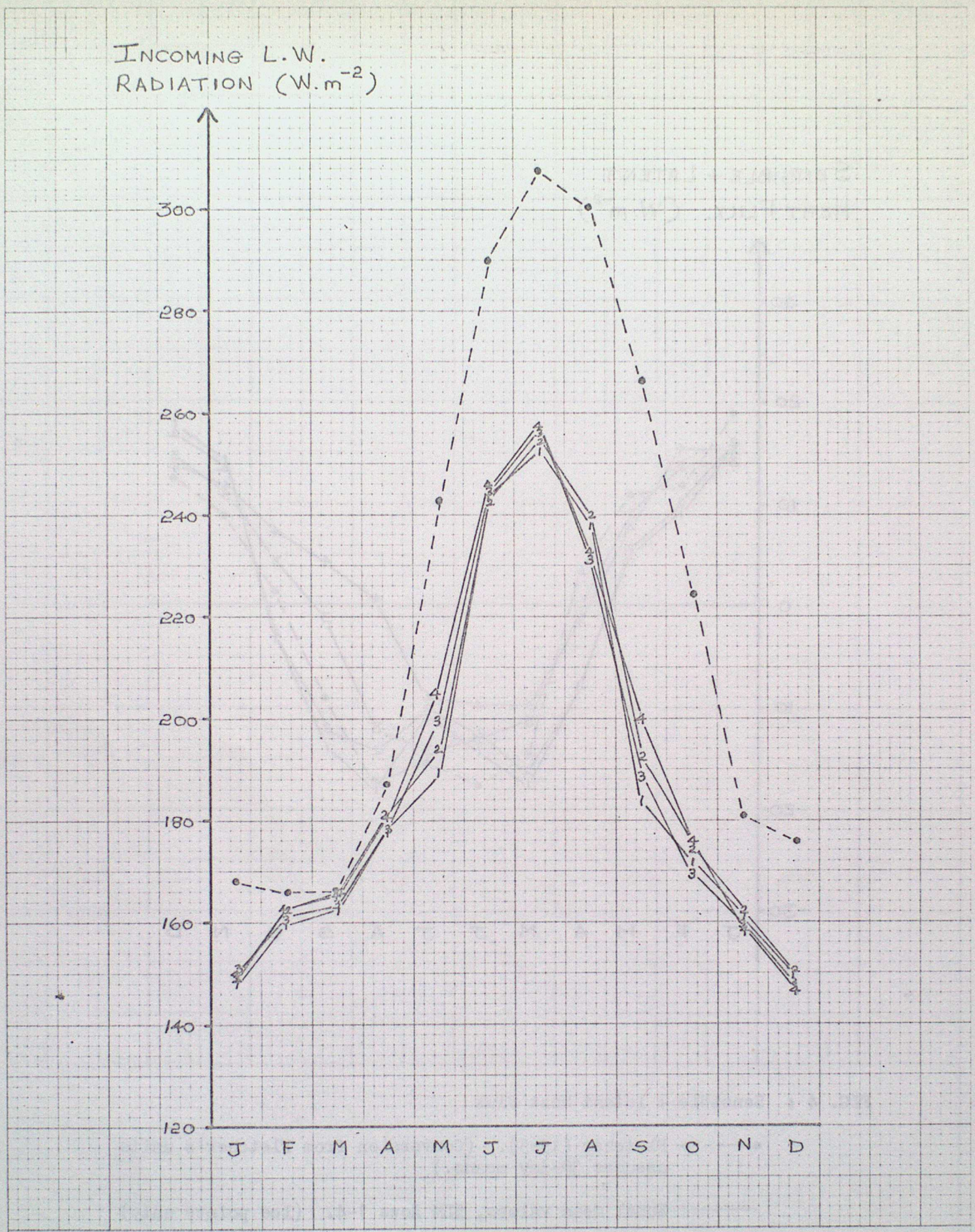

FIG. 3 : Incoming long-wave radiation

•------• Fletcher (1965). (Conversion from Fletcher's units assumes 30-day means.)

——— Zonal mean values, 5LM Rows 1-4. (Ice points only)

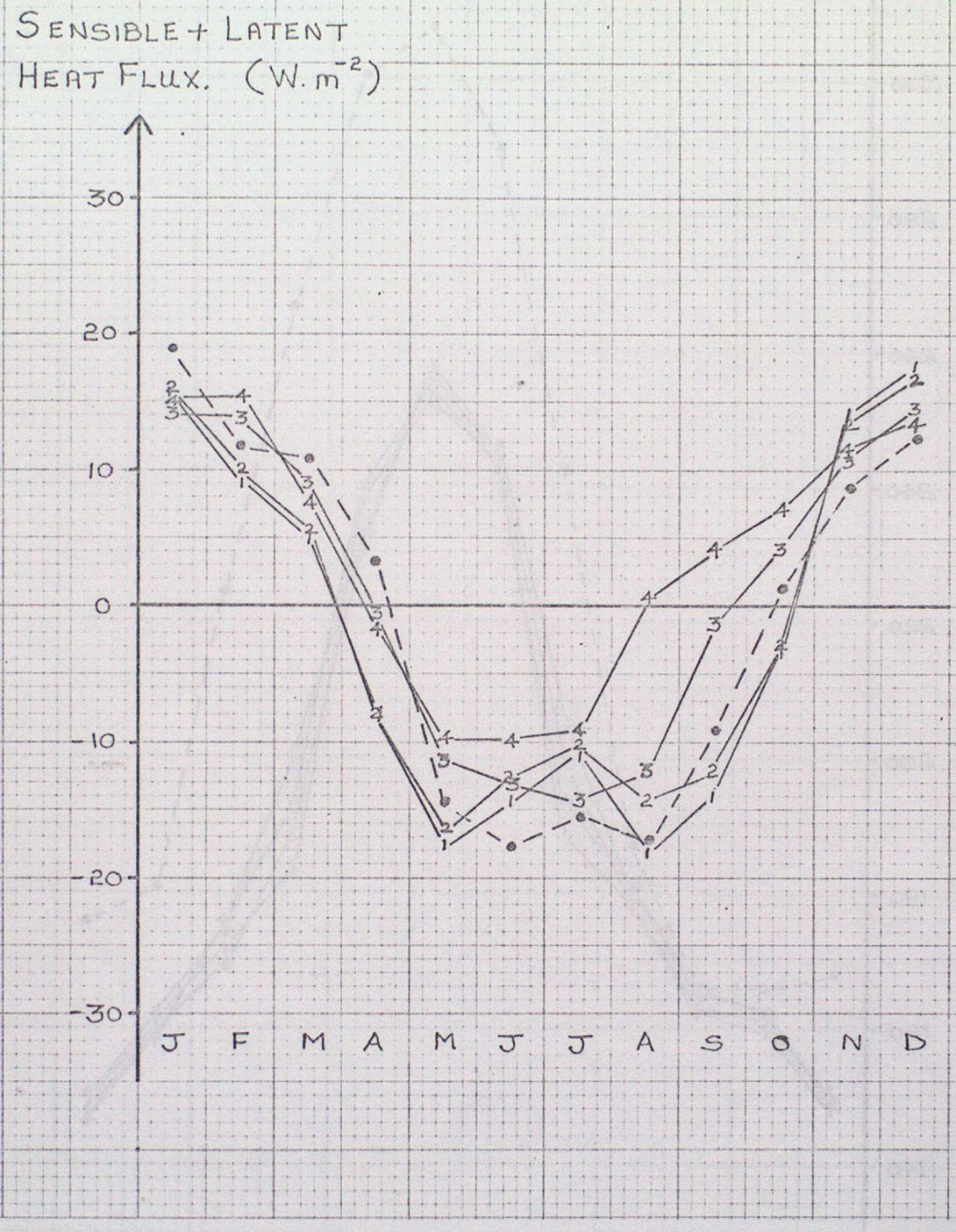

FIG. 4 : Sensible + latent heat flux

•------• Fletcher (1965). (Conversion from Fletcher's units assumes 30-day means.)

——— Zonal mean values, 5LM Rows 1-4. (Ice points only)

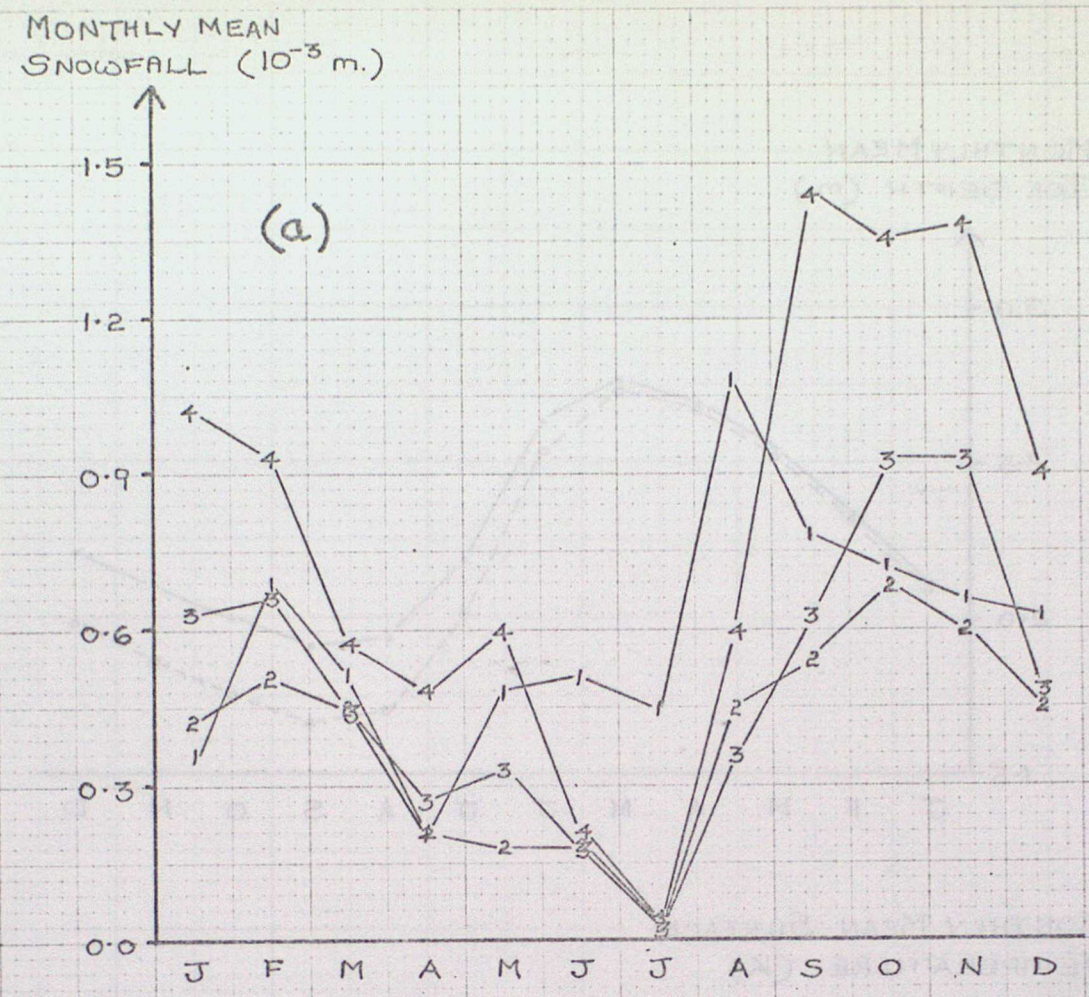

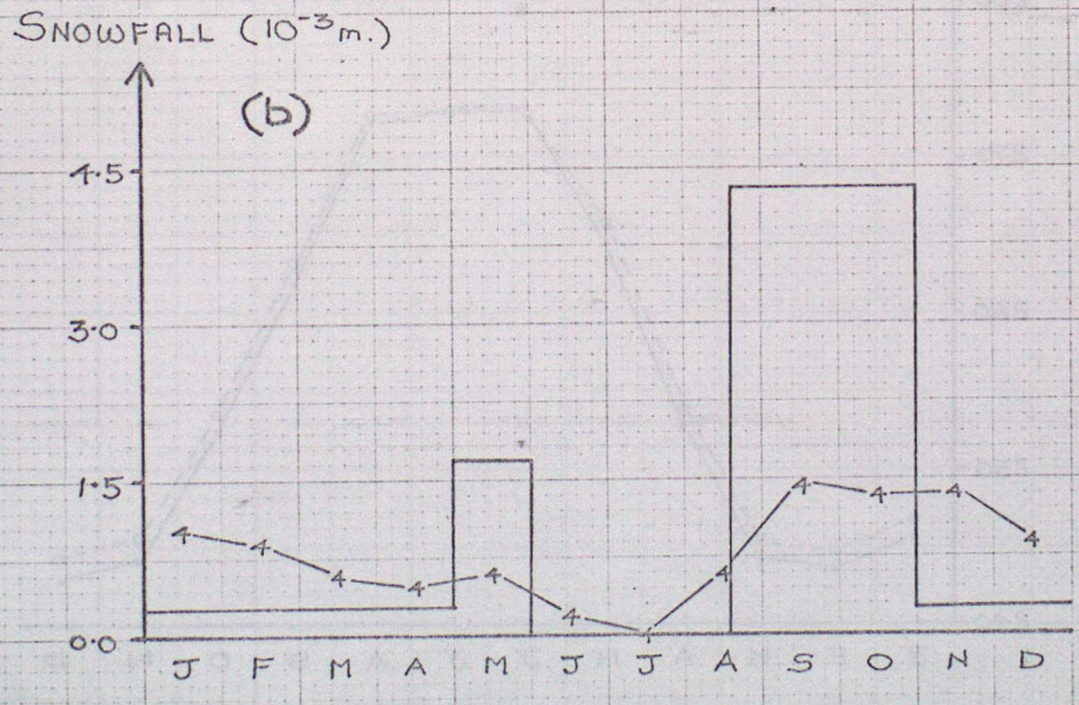

Fig 5: (a) Zonal mean GCM snowfall for Rows 1–4. (Ice points only).
(Factor of 3 x 10^{-3} used to convert from 5LM units of mm water equivalent).

(b) Comparison of Semtner snowfall with Row 4 zonal mean snowfall.

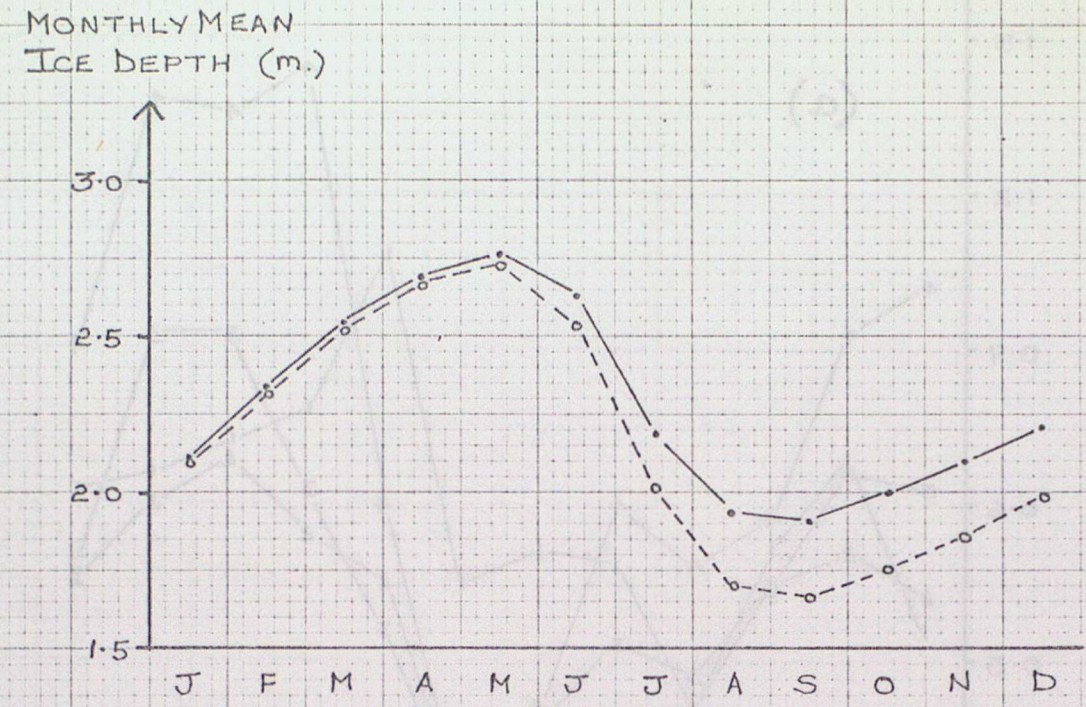

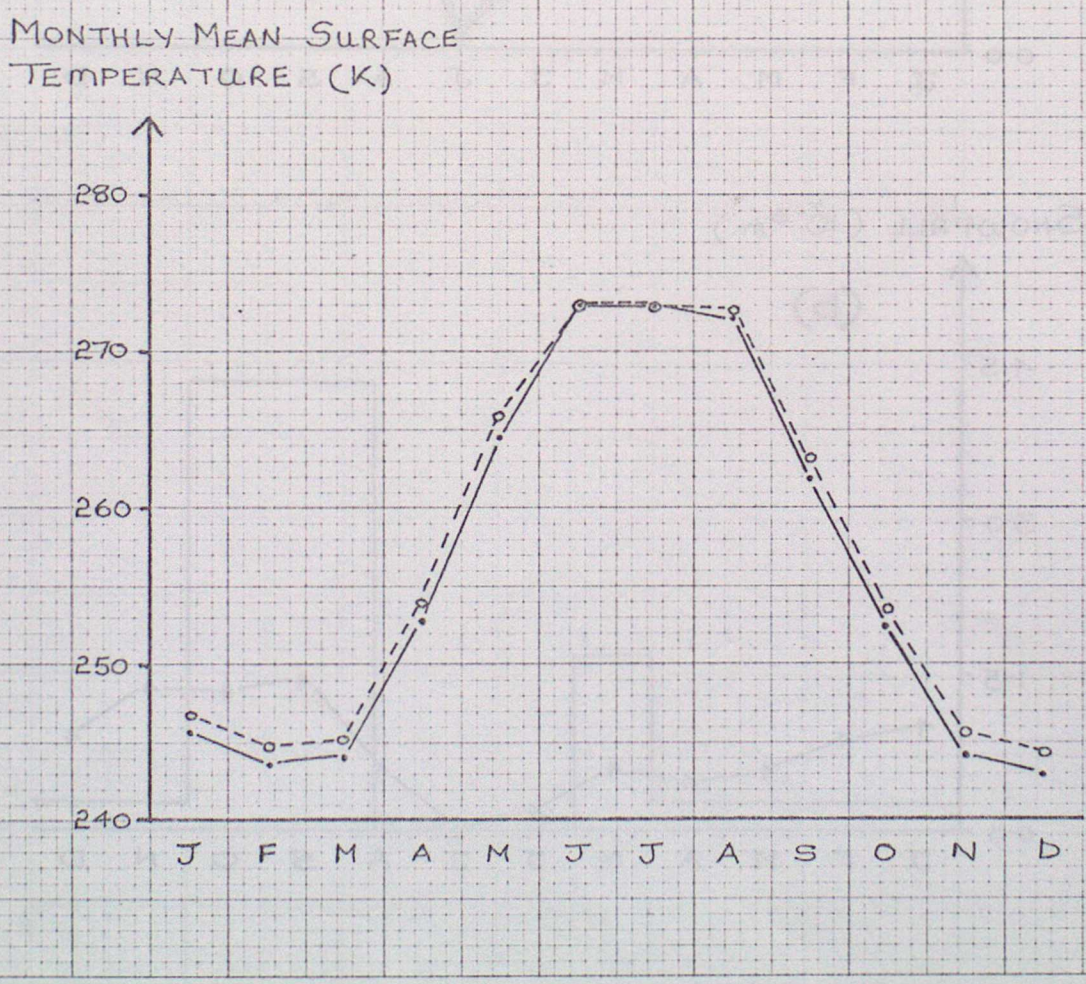

Fig 6: Monthly mean ice depth and surface temperature in the first year of Semtner's Case 1 integration (o———o) and in the corresponding calculation using the standard value of σ (o- - - - -o).

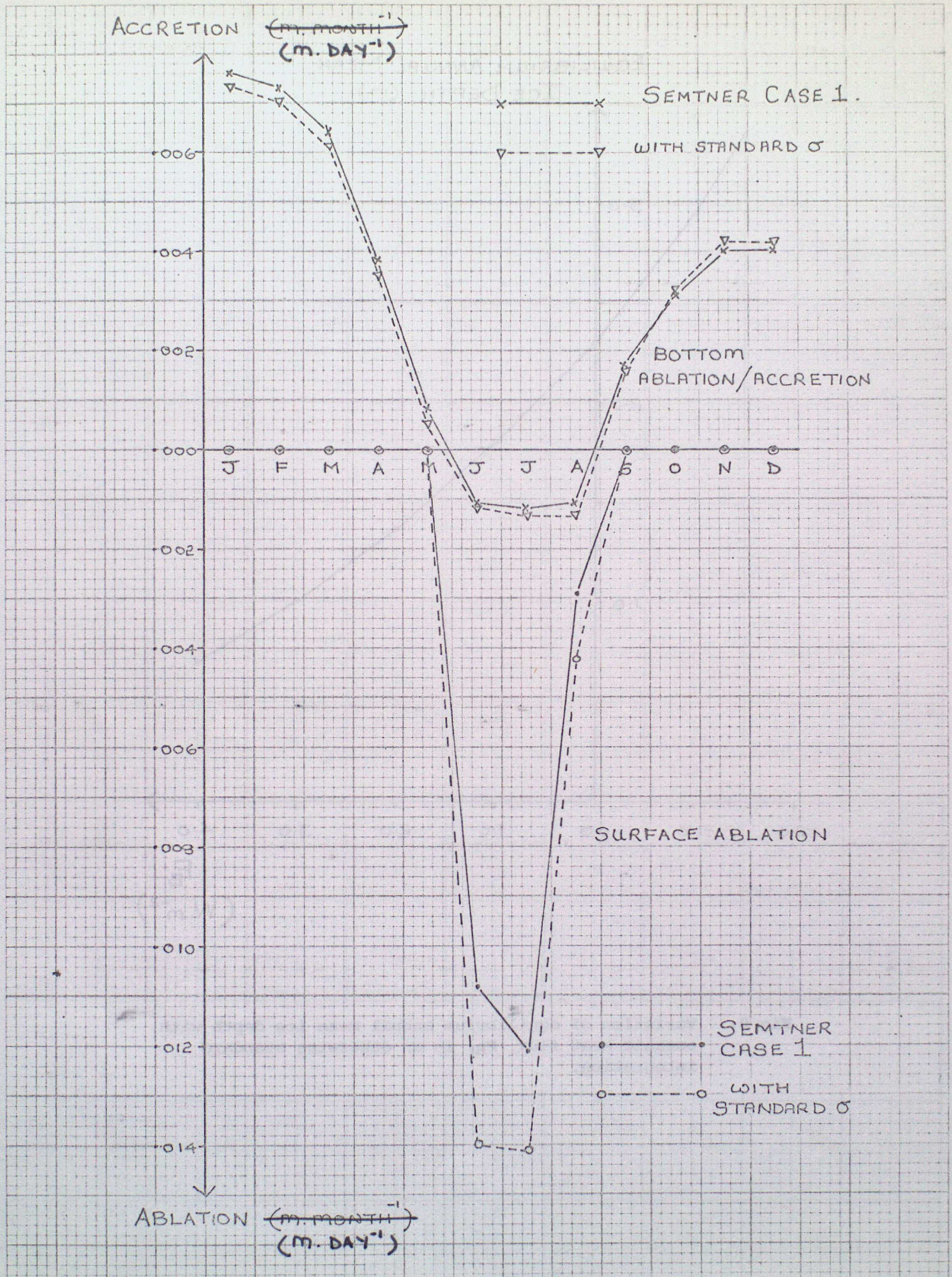

Fig 7: Contributions to the total change in ice depth from bottom ablation/accretion and surface ablation in the first year of Semtner's Case 1 integration and in the corresponding calculation using the standard value of σ.

96-0-0 A.G. 21/10569

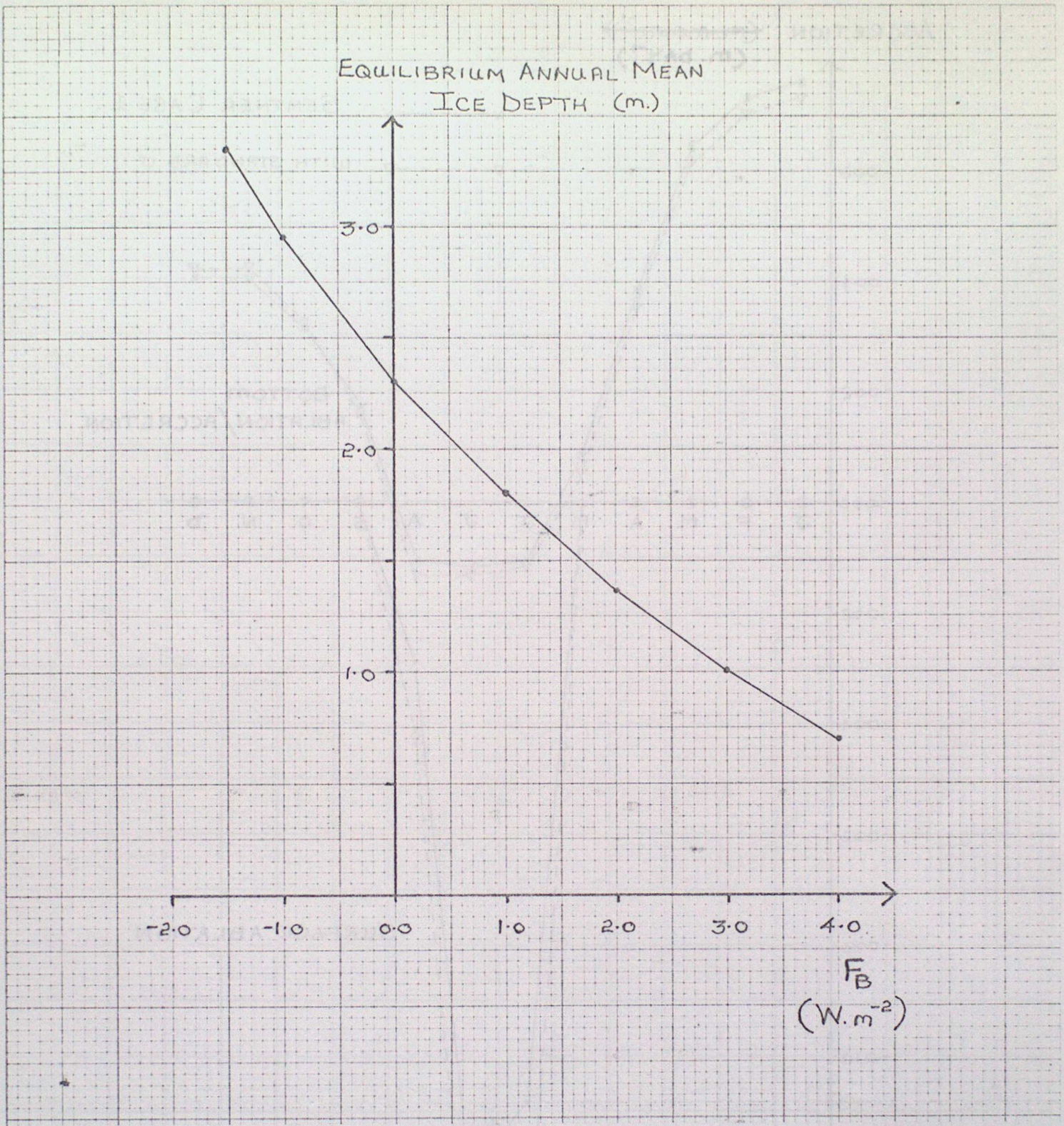

Fig 8: Variation of equilibrium annual mean ice depth with oceanic heat flux, F_B, in an otherwise standard integration.

Fig 9: Evolution of ice depth in the standard integration of the zero layer model. The broken horizontal lines show the annual mean ice depths.

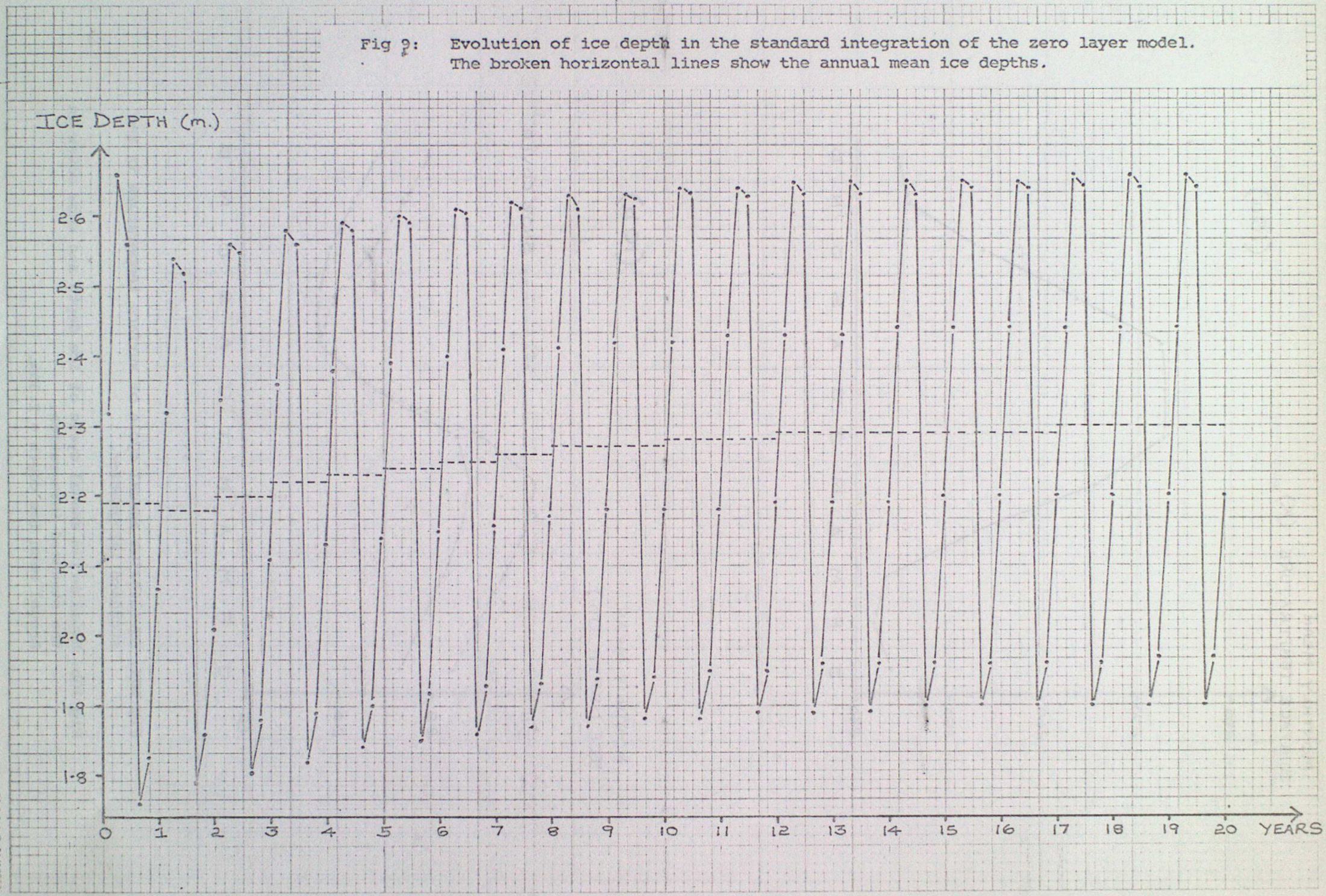

96·0·0 A.G. 21/10569

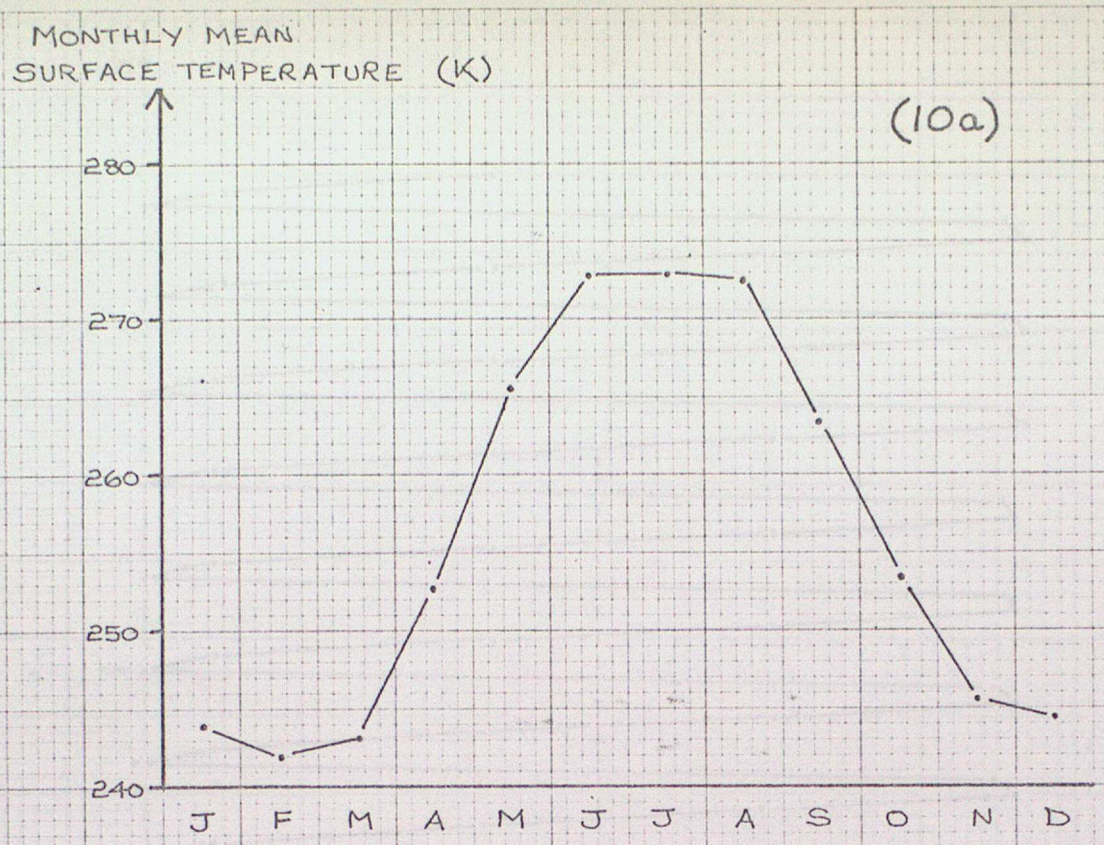

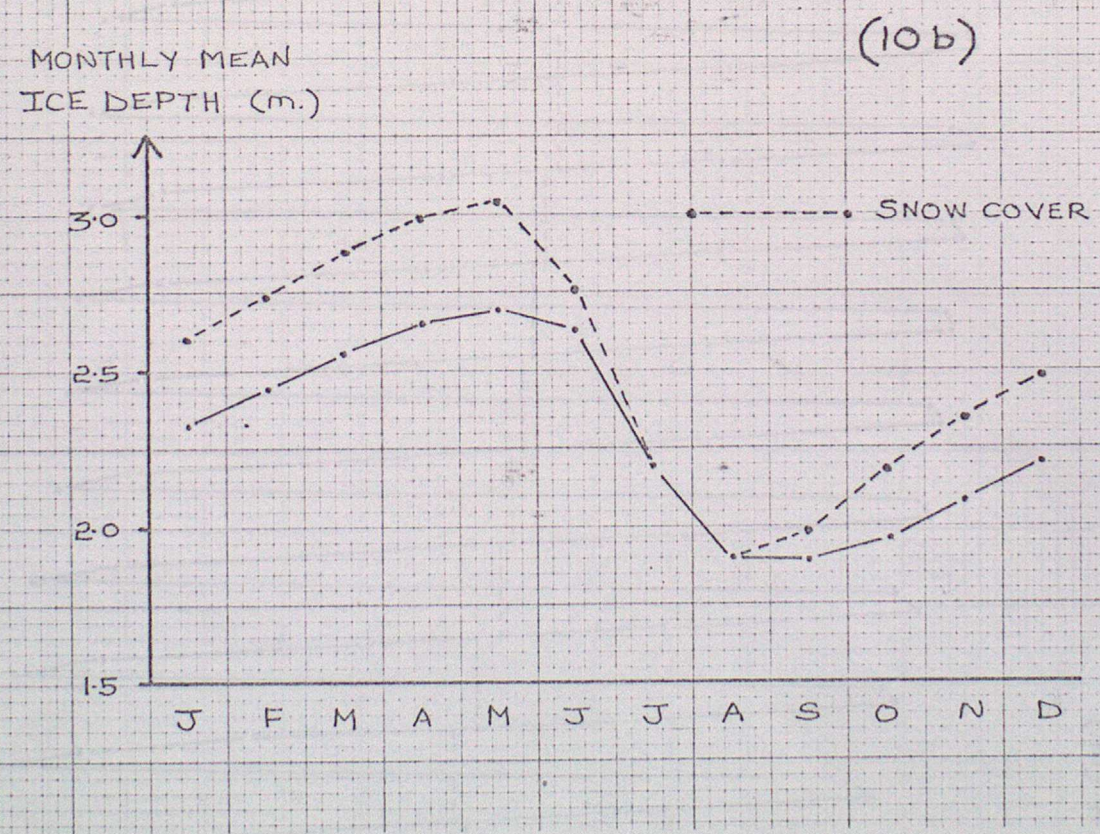

Fig 10a: Equilibrium annual cycle of surface temperature in the standard integration.

Fig 10b: Equilibrium annual cycle of ice depth and snow cover in the standard integration.
Annual mean ice depth = 2.30m.

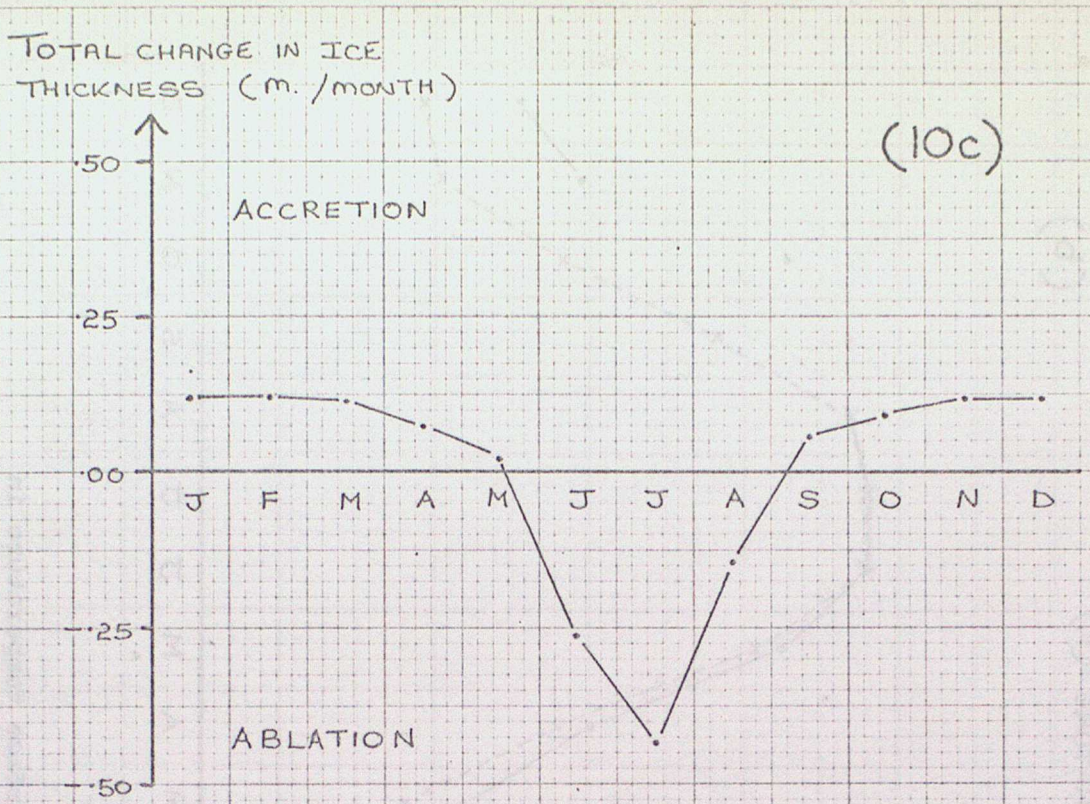

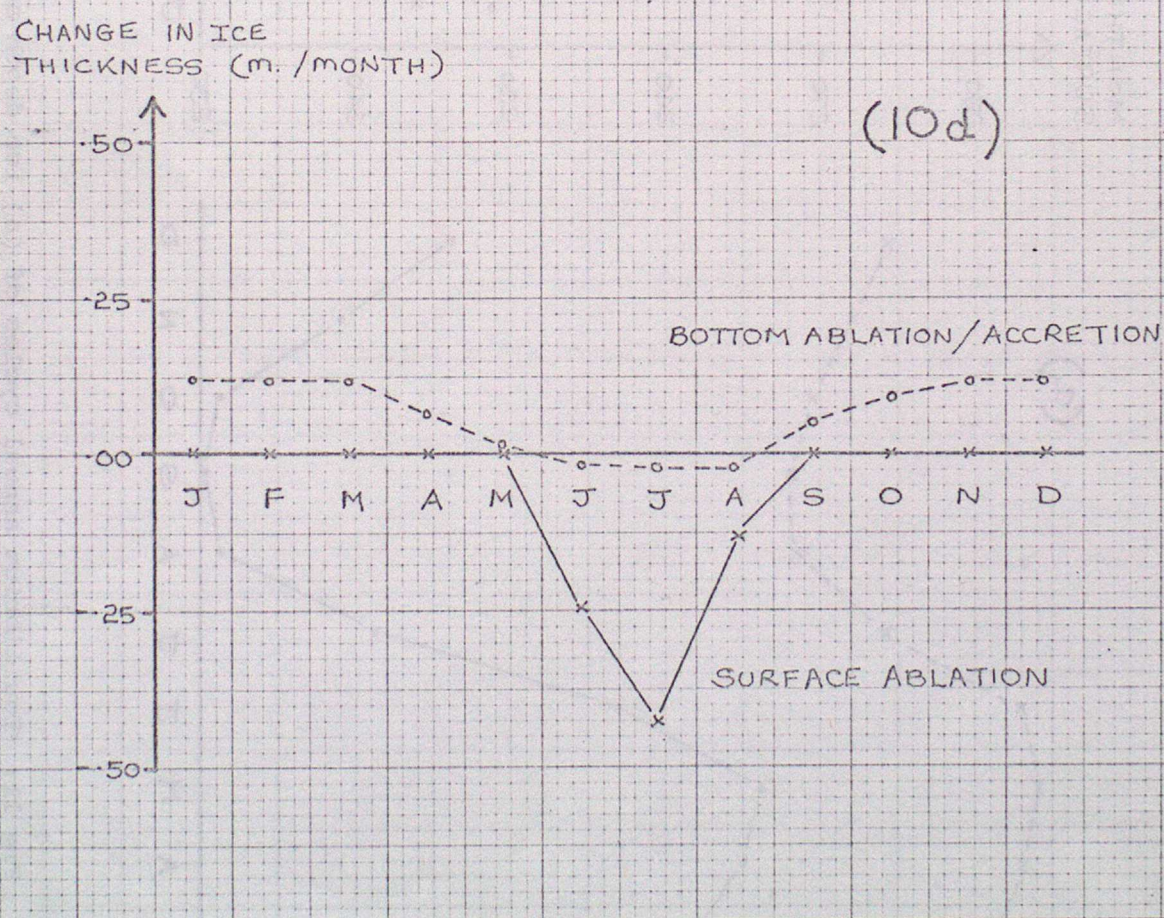

Fig 10c: Equilibrium annual cycle of total change in ice thickness in the standard integration.

Fig 10d: Contributions to the total change (shown in Fig. 10c) from bottom ablation/accretion (o-----o) and surface ablation (×———×).

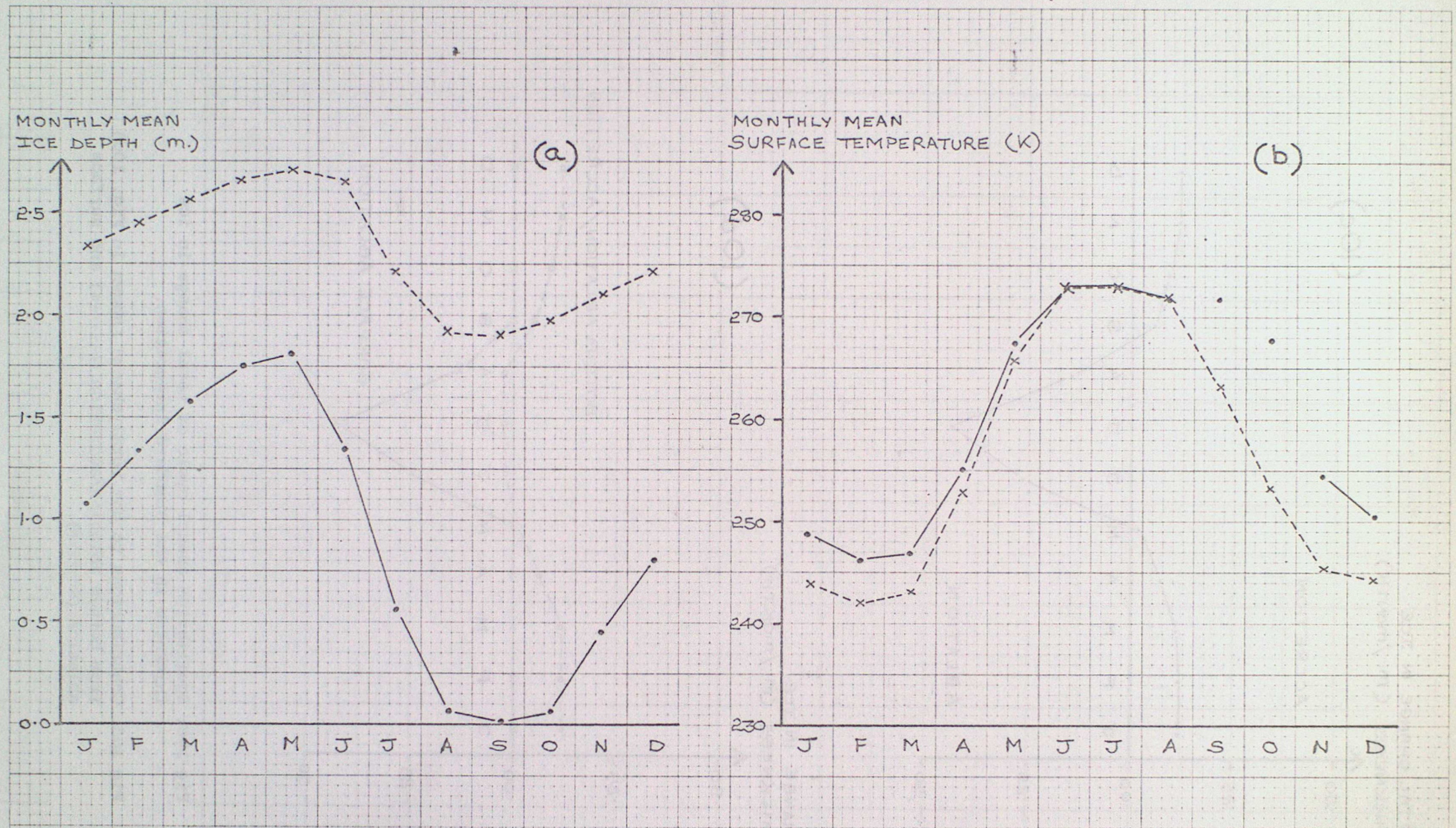

Fig 11: Equilibrium annual cycles of (a) ice depth and (b) surface temperature in the standard integration + 5LM albedo (•———•). (see section 5.2). Monthly mean surface temperatures for Aug, Sep and Oct are affected by the temperature of the mixed layer ocean during the period of open water. The broken line (×-----×) shows the corresponding cycles for the standard integration.

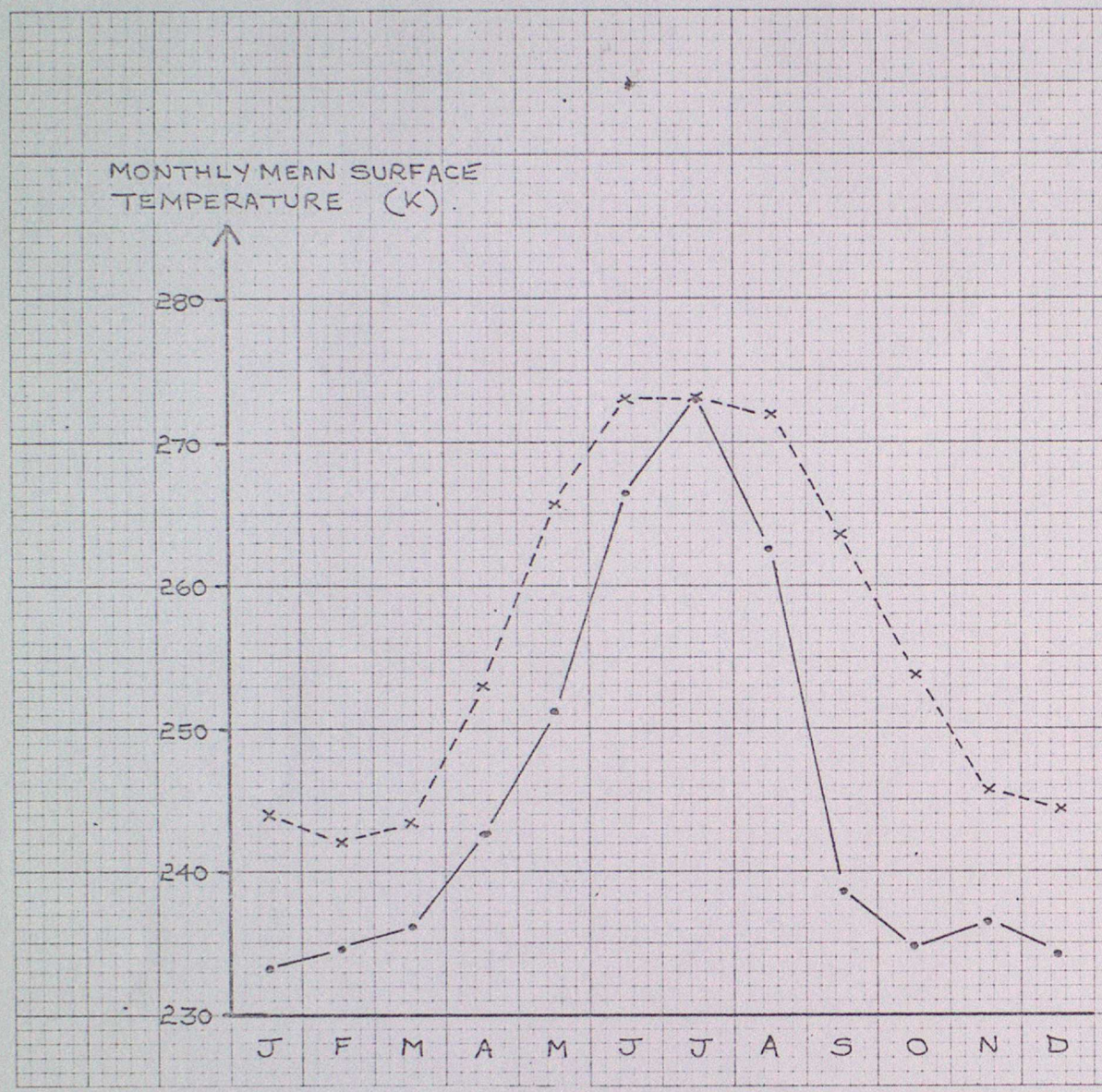

Fig 12: Variation of monthly mean surface temperature (•——•) in the final year (year 50) of the integration using Row 1 forcing + Semtner albedos (see section 6.1). The broken line (x----x) shows the equilibrium annual cycle of surface temperature in the standard integration.

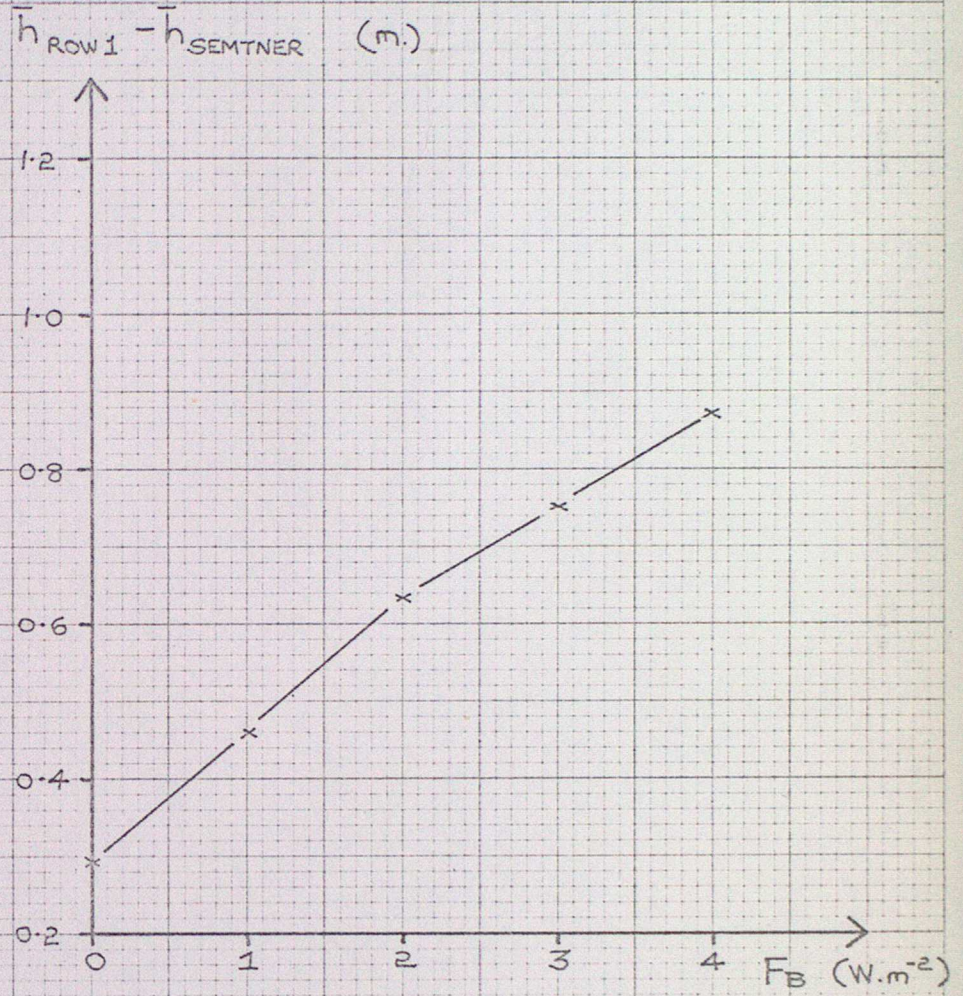

Fig 13: Sensitivity of model results to snowfall expressed as a function of oceanic heat flux, F_B. The vertical coordinate is the change in equilibrium annual mean ice depth (h) obtained on substituting Row 1 snowfall for Semtner snowfall.